RSK2 protects mice against TNF-induced bone loss

Christina Böhm[1,*], Anja Derer[1,*], Roland Axmann[1], Ulrike Hillienhoff[2], Mario M. Zaiss[1], Julia Luther[1], Christine Zech[1], Michael Stock[1], Carina Scholtysek[1], Klaus Engelke[3], Andreas Hess[4], Jan P. Tuckermann[2], Georg Schett[1] and Jean-Pierre David[1,‡]

[1]Internal Medicine 3, Rheumatology and Immunology, University of Erlangen-Nuremberg, Krankenhausstrasse 12, D-91054 Erlangen, Germany
[2]Molecular Biology of Tissue-specific Hormone Action, Leibniz Institute for Age Research, Fritz Lipmann Institute e.V., Beutenbergstrasse 11, D-07745 Jena, Germany
[3]Institute of Medical Physics, University of Erlangen-Nuremberg, Henkestrasse 91, D-91052 Erlangen, Germany
[4]Institute of Experimental and Clinical Pharmacology and Toxicology, University of Erlangen-Nuremberg, Fahrstrasse 17, D-91054 Erlangen, Germany

*These authors contributed equally to this work
‡Author for correspondence (j.david@uke.de)

Accepted 16 December 2011
Journal of Cell Science 125, 2160–2171
© 2012. Published by The Company of Biologists Ltd
doi: 10.1242/jcs.096008

Summary

Tumor necrosis factor (TNF)-α is a key cytokine regulator of bone and mediates inflammatory bone loss. The molecular signaling that regulates bone loss downstream of TNF-α is poorly defined. Here, we demonstrate that inactivating the pro-osteoblastogenic ERK-activated ribosomal S6 kinase RSK2 leads to a drastically accelerated and amplified systemic bone loss in mice ectopically expressing TNF-α [human TNF transgenic (*hTNF*tg) mice]. The phenotype is associated with a decrease in bone formation because of fewer osteoblasts as well as a drastically increased bone destruction by osteoclasts. The molecular basis of this phenotype is a cell autonomous increased sensitivity of osteoblasts and osteocytes to TNF-induced apoptosis combined with an enhancement of their osteoclast supportive activity. Thus, RSK2 exerts a strong negative regulatory loop on TNF-induced bone loss.

Key words: RSK2, TNF-α, Osteopenia, TNF, Apoptosis, Osteoblast, Osteocyte

Introduction

Bone is one of the tissues that can regenerate in adult mammals as a consequence of the permanent bone remodeling. This process allows a proper maintenance of bone homeostasis as well as tissue repair that maintains the integrity of the adult bone. Bone remodeling is orchestrated by the combined activities of three major cell types, the osteoclasts, the osteoblasts and the osteocytes (Bonewald, 2011; Bruzzaniti and Baron, 2006; Karsenty et al., 2009; Teitelbaum and Ross, 2003). A central player is the osteocyte that is the latest stage of differentiation of the osteoblastic bone-forming cells. These cells that make up more than 90% of bone cells are embedded into the mineralized bone and form a complex network of ramified connections, disruption of which is believed to serve as sensor to initiate cycles of bone remodeling (Bonewald, 2011). Indeed, disruption of the osteocyte network as a consequence of apoptosis sends signals (which have not yet been identified) for the recruitment of the bone resorbing cells (the osteoclasts). Following resorption of the damaged bone by osteoclasts, mesenchymal osteoblasts move in, secreting bone matrix proteins and mineralizing the osteoids to regenerate bone. As a result, some osteoblasts are trapped in the newly formed bone matrix and terminally differentiate into osteocytes that negatively regulate both osteoclast and osteoblast activities, switching off the remodeling cycle (Jilka et al., 2007; Nakahama, 2010; Raggatt and Partridge, 2010).

Any disruption of this equilibrium leads to the development of bone pathologies such as age-related bone loss, post-menopausal osteoporosis and inflammatory bone loss. A pro-inflammatory cytokine, tumor necrosis factor-α (TNF-α) is believed to be a central mediator of systemic bone loss by interfering with the bone remodeling cycle (David and Schett, 2010; Nanes, 2003). This concept is highlighted by rheumatoid arthritis where anti-TNF therapy represents one of the most efficient protective treatments against bone loss (Schett and David, 2010; Sfikakis, 2010) as well as in postmenopausal osteoporosis (Charatcharoenwitthaya et al., 2007). Clinical studies have also correlated the progression of postmenopausal osteoporosis with increased levels of circulating TNF-α in postmenopausal women (Pacifici, 2008). The central role of TNF-α in postmenopausal osteoporosis was further demonstrated in the classical mouse model of ovariectomy where TNF-α and TNF-α-receptor-1 (TNF-R1; also known as TNFRSF1A)-deficient mice were both protected against bone loss resulting from estrogen depletion (Roggia et al., 2001). In addition to its function in inducing pathological bone loss, TNF-α appears to be a physiological regulator of bone homeostasis, by slowing down bone formation by osteoblasts (Li et al., 2007).

At the cellular level, local or systemic increase in the concentration of TNF-α leads to complex deregulation of bone remodeling that not only favors bone destruction by increasing osteoclasts differentiation and activation, but also inhibits bone formation by blocking differentiation and activity of osteoblasts as well as inducing their apoptosis (David and Schett, 2010; Nanes, 2003). In addition, a high level of apoptosis of osteocytes is also a recognized consequence of TNF-α stimulation (Plotkin et al., 1999). At the molecular level, TNF-α acts primarily through TNF-RI to directly enhance osteoclast differentiation in response to macrophage-colony-stimulating factor (M-CSF; also known as CSF1) and receptor activator of NF-κB ligand

Journal of Cell Science

Journal of Cell Science

(RANKL; also known as tumor necrosis factor ligand superfamily member 11; TNFSF11) (Abu-Amer et al., 2000; Zhang et al., 2001) and to indirectly induce the secretion of pro-osteoclastogenic cytokines by supportive osteoblastic cells (Hofbauer et al., 1999; Thomson et al., 1987). TNF-α also acts directly on osteoblasts through TNF-RI, by blocking the expression of the two essential osteoblastogenic transcription factors, runt-related transcription factor 2 (Runx2) and its downstream target osterix (Osx; also known as Sp7) and therefore inhibiting the differentiation of the cells (Gilbert et al., 2002; Lu et al., 2006). In addition, TNF-α binding to TNF-RI is a known activator of pro-apoptotic signals; however, the exact mechanism of TNF-induced apoptosis of osteoblasts in vivo is still unclear (Nanes, 2003).

We and others previously identified the ERK- and phosphoinositide 3-kinase-dependent kinase RSK2 as a regulator of bone formation in vivo. Indeed, RSK2-deficient mice recapitulated the progressive bone loss due to decreased bone mineralization by the osteoblasts observed in patients with Coffin–Lowry syndrome (CLS) (David et al., 2005; Marques Pereira et al., 2010; Yang et al., 2004). Although the differentiation of the cells in vitro was drastically blocked, the in vivo phenotype was clearly attributed to a cell autonomous decrease in the activity of the osteoblasts rather than a decrease in their numbers (David et al., 2005; Yang et al., 2004). Interestingly, RSK2 was recently shown to interact with TNF-RI, protecting HeLa cells from apoptosis induced by the combined stimulation with TNF-α and cyclohexamide (Peng et al., 2010). However, no in vivo demonstration of the role of RSK2 as a modulator of TNF-α has been reported.

Here, we demonstrate the exacerbation of TNF-induced bone loss in the absence of RSK2. This phenotype appears to be caused by an increased sensitivity of the osteoblastogenic cells to TNF-α.

Results

Severe growth retardation and early mortality of *hTNF*tg mice lacking RSK2

To analyze the potential role of RSK2 in mediating TNF-α effects on bone, we generated TNF-α-overexpressing mice lacking RSK2 (*hTNF*tg;*Rsk2*$^{-/y}$) by crossing *hTNF*tg mice (Keffer et al., 1991) with *Rsk2* knockout mice (David et al., 2005; Yang et al., 2004). Compared with all littermates of the various genotypes [wild-type (WT), *Rsk2*$^{-/y}$ and *hTNF*tg], 10-week-old *hTNF*tg;*Rsk2*$^{-/y}$ mice appeared severely growth retarded (Fig. 1A). We established the growth curves of the different genotypes and their wild-type littermates, which confirmed the known age-related loss in body weight of the *hTNF*tg mice as well as the mild decrease in the body weight of RSK2-deficient mice. Strikingly, RSK2-deficient *hTNF*tg mice barely gained any weight with age and appeared severely growth retarded at each point time (Fig. 1B). Although no mortality of wild-type or the *Rsk2*$^{-/y}$ mice was seen, none of the *hTNF*tg mice lived longer than 17 weeks and none of the RSK2-deficient *hTNF*tg mice lived longer than 11 weeks (Fig. 1C). Kaplan–Meier analysis estimated the half life of the *hTNF*tg mice at 16 weeks and of the RSK2-deficient *hTNF*tg mice at 10 weeks (Fig. 1C). Thus, compared with the *hTNF*tg mice, an earlier mortality and more severe growth retardation characterized RSK2-deficient *hTNF*tg mice, suggesting an increased sensitivity to the systemic effects of TNF-α in the absence of RSK2.

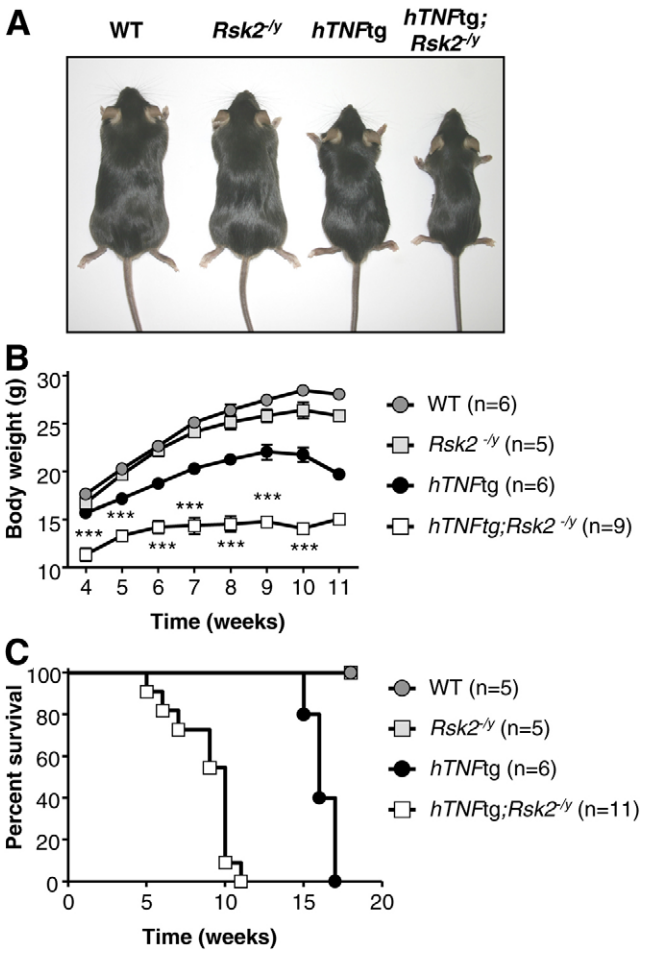

Fig. 1. The human TNF transgenic mice lacking RSK2 (*hTNF*tg;*Rsk2*$^{-/y}$) are severely growth retarded and show early lethality. (**A**) Representative 10-week-old male littermates of the genotypes, wild-type (WT), RSK2-deficient (*Rsk2*$^{-/y}$), human TNF transgenic (*hTNF*tg) and RSK2-deficient human TNF transgenic (*hTNF*tg;*Rsk2*$^{-/y}$) mice. (**B**) Body weight measurement of males of the indicated genotypes between weeks 4 and 11 (statistical analysis by two-way ANOVA comparing *hTNFtg;Rsk2*$^{-/y}$ with *hTNF*tg, ***$P<0.001$). (**C**) Kaplan–Meier survival curve of males of the indicated genotypes.

Severe osteopenia in *hTNF*tg mice lacking RSK2

Mice overexpressing hTNF developed severe progressive inflammatory arthritis leading to local and systemic bone destruction (Keffer et al., 1991). Interestingly, deletion of RSK2 led to an earlier onset of all the clinical signs of arthritis as well as of an exacerbation of TNF-induced local joint destruction (data not shown).

The inflammation-driven osteopenia observed in *hTNF*tg mice (Schett et al., 2003) and the aged-dependent bone loss of *Rsk2*$^{-/y}$ mice (David et al., 2005) prompted us to focus our analysis on the bone of RSK2-deficient *hTNF*tg mice. Histological analysis of bone sections in tibiae by von Kossa staining showed no substantial change in 6-week-old *Rsk2*$^{-/y}$ mice, but the expected slightly decreased bone mass of the *hTNF*tg mice was drastically amplified in RSK2-deficient *hTNF*tg mice (Fig. 2A), leading to a very reduced trabecular structure at 10 weeks of age (Fig. 2B). These observations were quantitatively confirmed by histomorphometry that indicated a drastic and early decrease in

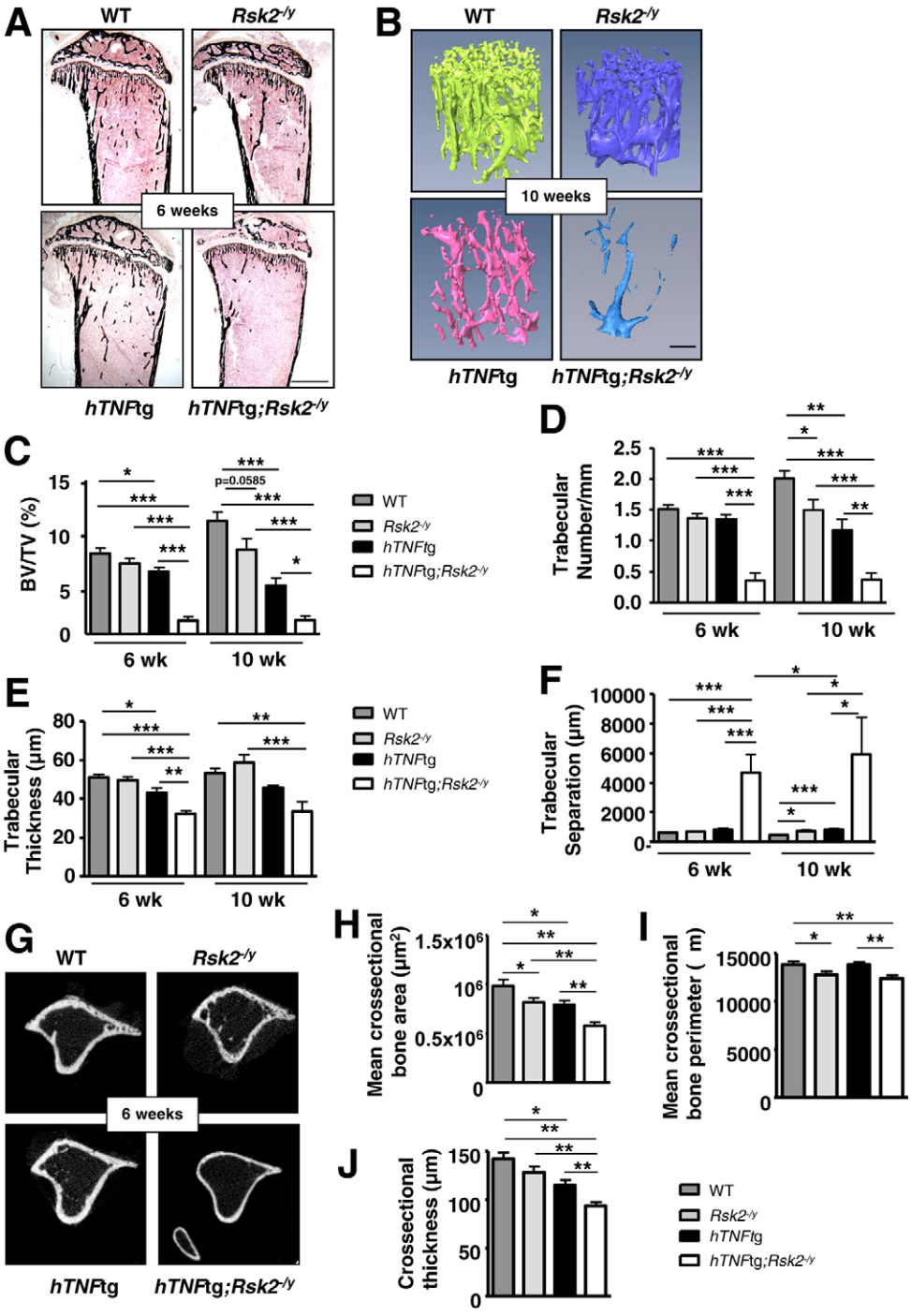

Fig. 2. Severe osteopenia in *hTNF*tg;*Rsk2*$^{-/y}$ mice. (**A**) Von Kossa staining of undecalcified tibiae from 6-week-old males of the indicated genotypes. Scale bar: 500 µm. (**B**) Micro-computer tomography analysis of trabecular bone from 10-week-old males. Scale bar: 250 µm. (**C–F**) Histomorphometry of the bone of 6- and 10-week-old males (n=8–11): quantification of bone volume relative to total volume (BV/TV) (C); trabecular number (D); trabecular thickness (E); and trabecular separation (F). Values are means ± s.e.m. *P<0.05, **P<0.01, ***P<0.001. (**G**) Micro-computer tomography analysis of cortical bone from 6-week-old males of the indicated genotypes (n=4–9). (**H–J**) Quantification of the cortical area (H), the cortical bone perimeter (I) and cortical bone thickness (J). Values are means ± s.e.m. *P<0.05, **P<0.01, ***P<0.001.

bone volume in RSK2-deficient *hTNF*tg mice (Fig. 2C). The phenotype was associated with significantly (P<0.05) fewer (Fig. 2D), thinner (Fig. 2E) and more separated (Fig. 2F) trabeculae. We previously reported decreased cortical bone volume in RSK2-deficient mice (David et al., 2005). We therefore performed micro-computer tomography (microCT) on the cortical bone of 6-week-old mice that indicated an even lower cortical bone volume in RSK2-deficient *hTNF*tg mice (Fig. 2G). Quantitative comparison of the cortical bone parameters confirmed the lower cortical bone in RSK2-deficient mice as well as in *hTNF*tg mice that was further amplified in the combined RSK2-deficient *hTNF*tg mice, resulting in thinner cortical bone (Fig. 2H–J). Thus, inactivating RSK2 resulted in earlier and more profound TNF-mediated bone loss.

Lower trabecular and periosteal bone formation in *hTNF*tg mice lacking RSK2

Because decreased bone formation is observed in aging RSK2-deficient mice (David et al., 2005) and TNF-α is a known inhibitor of osteoblast activity (David and Schett, 2010; Nanes, 2003), we hypothesized that inactivating RSK2 in *hTNF*tg mice would result in an exacerbation of TNF-mediated blockage of

bone formation. We performed dynamic histomorphometry following double injection of Calcein to quantitatively compare the kinetic of bone formation between the four groups of mice at 6 weeks of age. Although no changes in the dynamic parameters of endosteal bone formation was measured in any of the mice (supplementary material Fig. S1A,B), a drastic decrease in the bone formation rate (BFR) due to a combined decrease in the mineral apposition rate (MAR) and in the mineralized surface per bone surface (MS/BS) was seen in both periosteal and trabecular bone of the RSK2-deficient *hTNF*tg mice (supplementary material Fig. S1C–F).

Lower osteoblast and higher osteoclast numbers in *hTNF*tg mice lacking RSK2

We next performed bone histomorphometry in 6- and 10-week-old mice in order to better characterize the cellular origin of the bone phenotype of the RSK2-deficient *hTNF*tg mice. As expected, the number of osteoblasts in 10-week-old *hTNF*tg mice was slightly lower than in wild-type mice and this phenotype was amplified in RSK2-deficient *hTNF*tg mice (Fig. 3C,E). Similarly, the expected higher osteoclast parameters were seen in the 10-week-old *hTNF*tg mice, which were also amplified in the RSK2-deficient *hTNF*tg mice (Fig. 3F,H,J). Interestingly, whereas at 6 weeks of age no clear difference in the osteoblast and osteoclast parameters could be measured in the $Rsk2^{-/y}$ and *hTNF*tg mice, 6-week-old *hTNF*tg;$Rsk2^{-/y}$ mice did exhibit a strong reduction in the number of osteoblasts and in osteoblast-covered surface, as well as a drastic increase in the number of osteoclasts and in osteoclast-covered surface (Fig. 3A, B, D, G and I). Thus, the much reduced bone in RSK2-deficient *hTNF*tg mice is probably due to lower osteoblast numbers and higher osteoclast numbers early in development.

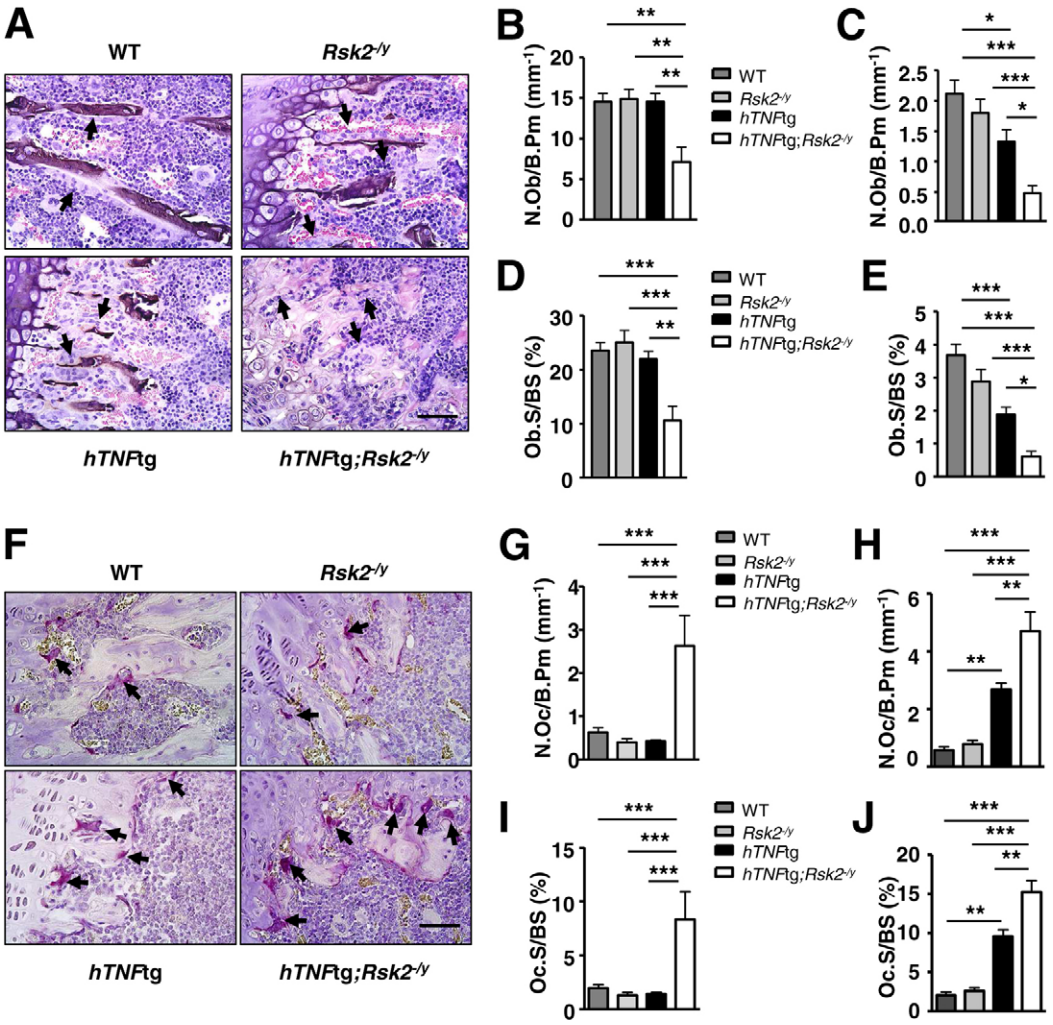

Fig. 3. Osteoblast and osteoclast numbers in *hTNF*tg mice lacking RSK2. (**A**) Hematoxylin and Eosin staining of undecalcified sections of tibiae from 6-week-old males of the indicated genotypes. Osteoblasts are indicated by black arrows. Scale bar: 25 µm. (**B–E**) Histomorphometric quantification of osteoblast numbers relative to bone perimeter (N.Ob/B.Pm) at 6 (B) and 10 (C) weeks of age, and osteoblast covered surface normalized to bone surface (Ob.S/BS) of 6- (D) and 10- (E) week-old mice (n=7–9 mice). (**F**) TRAP staining of paraffin sections of tibiae from 10-week-old males. Black arrows indicate osteoclasts. Scale bar: 25 µm. (**G–J**) Histomorphometric assessment of osteoclast numbers per bone perimeter (N.Oc/B.Pm) at 6 (G) and 10 (H) weeks of age and osteoclast-covered surface normalized to bone surface (Oc.S/BS) of 6- (**I**) and 10- (**J**) week-old males (n=7–12). Values are means ± s.e.m. *P<0.05, **P<0.01, ***P<0.001.

Increased osteoclastogenic supportive activity of RSK2-deficient osteoblasts

A similar level of circulating RANKL and a slightly higher level of circulating OPG were detected in the serum of RSK2-deficient *hTNF* transgenic mice (supplementary material Fig. S2A,B), suggesting that a change in the ratio of circulating RANKL/OPG could not explain the higher osteoclast numbers observed in vivo. We next transferred the bone marrow of RSK2-deficient or wild-type mice into *hTNF* transgenic mice to determine whether the more severe bone destruction in the absence of RSK2 could be due to a cell autonomous increased susceptibility of hematopoietic cells to the pro-osteoclastogenic environment. Bone loss was unchanged in *hTNF*tg mice receiving RSK2-deficient bone marrow when compared with wild-type bone marrow cells (Fig. 4A). Moreover, histomorphometric analysis of osteoclasts parameters in the tibia did not reveal any difference between the two groups. These results strongly suggested that the higher osteoclast numbers seen in RSK2-deficient *hTNF* transgenic mice was not due to a cell autonomous defect in the osteoclast lineage lacking RSK2 (Fig. 4B). We therefore performed in vitro osteoclastogenesis to test this hypothesis. As expected, no difference in the osteoclast differentiation or in

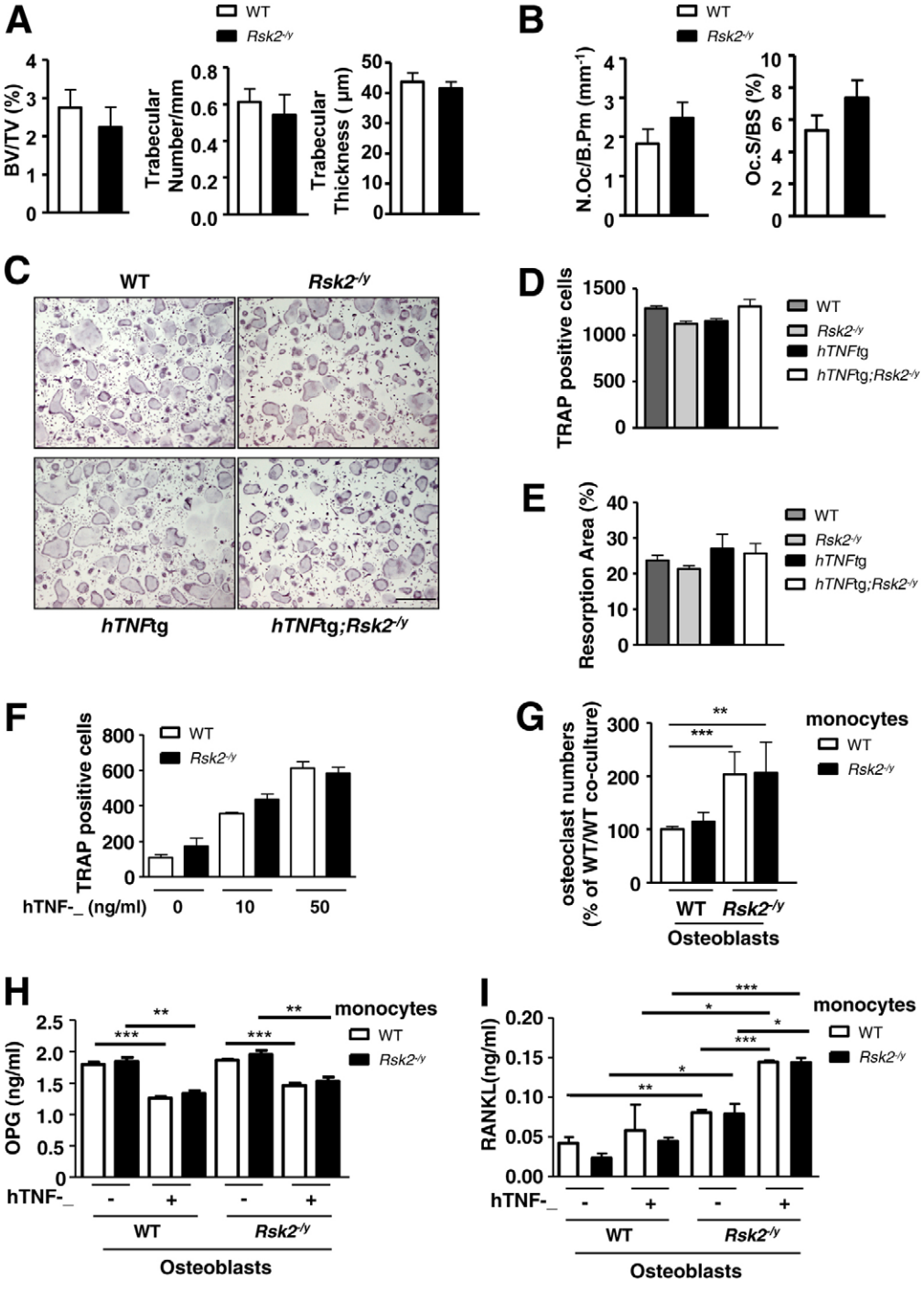

Fig. 4. There is no cell intrinsic alteration in osteoclastogenesis in *hTNF*tg mice lacking RSK2 but increased pro-osteoclastogenic function of RSK2-deficient osteoblasts. (**A**) Histomorphometric analysis of bone parameters: BV/TV, trabecular numbers and thickness, of *hTNF*tg mice following transfer of the bone marrow of wild-type or *Rsk2*$^{-/y}$ mice. (**B**) Histomorphometric quantification of osteoclast parameters in the mice with the transferred bone marrow. (**C**) Bone-marrow-derived cells of the indicated phenotype were cultured for 5 days in the presence of M-CSF (30 ng/ml) and RANKL (10 ng/ml) to promote osteoclast differentiation. Cells were fixed and stained for TRAP (tartrate-resistant acid phosphatase). Multinucleated purple cells are osteoclasts. Scale bar: 250 µm. (**D**) Assessment of TRAP-positive osteoclasts in the same culture condition. (**E**) Osteoclast precursors were plated on Osteologic^{TM} plates to quantify resorptive activity of osteoclasts. (**F**) Quantification of TRAP-positive cells from osteoclast differentiation of WT and RSK2-deficient monocytes cultured in the presence of permissive dose of RANKL (1 ng/ml) and increasing doses of hTNF-α. (**G**) Quantification of TRAP-positive cells in co-culture of wild-type or *Rsk2*$^{-/y}$ osteoblasts with wild-type or *Rsk2*$^{-/y}$ monocytes. (**H**,**I**) ELISA measurement of OPG (H) or RANKL (I) in the supernatant at day 2 of co-culture in the absence (−) or presence (+) of 10 ng/ml of TNF-α.

Journal of Cell Science

their resorptive activity between wild-type and RSK2-deficient monocytes could be seen in response to the two essential osteoclastogenic cytokines M-CSF and RANKL (Fig. 4C–E), and, more surprisingly, in response to TNF-α in the presence of a permissive amount of RANKL (Fig. 4F). Thus, we conclude that RSK2 deficiency does not directly affect osteoclastogenesis in vivo. We performed co-culture experiments to test whether an increased pro-ostoclastogenic activity of RSK2-deficient osteoblasts could explain the higher osteoclast numbers in vivo in *hTNF*tg mice lacking RSK2. Although, as expected, no difference in the numbers of osteoclast was observed in co-culture of wild-type osteoblasts with wild-type or RSK2-deficient monocytes, a twofold increase in osteoclast numbers was consistently observed when using RSK2-deficient osteoblasts (Fig. 4G). We therefore measured the levels of OPG and RANKL secreted into the supernatant by osteoblasts grown in co-culture conditions. No difference in the levels of OPG was found (Fig. 4H), but an increase in the level of secreted RANKL was detected in co-culture of RSK2-deficient osteoblasts compared with wild-type cells (Fig. 4I). In addition, although the secretion of OPG was similarly downregulated in response to TNF-α in both co-cultures of wild-type or RSK2-deficient osteoblasts with wild-type or RSK2-deficient monocytes (Fig. 4H), a further increase in the levels of secreted RANKL was observed in TNF-α-stimulated RSK2-deficient, but not wild-type, osteoblasts (Fig. 4G). Thus, an increased pro-osteoclastogenic activity of osteoblasts lacking RSK2 as a consequence of increased RANKL synthesis could at least partly explain the higher number of osteoclasts observed in RSK2-deficient *hTNF* transgenic mice. In agreement, a significantly ($P<0.001$) increased expression of RANKL mRNA but not of OPG was found in osteoblasts lacking RSK2 and overexpressing human TNF (supplementary material Fig. 2C,D).

Decreased expression of osteoblast and osteocyte markers in the long bones of *hTNF*tg mice lacking RSK2

We observed a mild, albeit non significant, decrease in the weight and size of 3-day-old RSK2-deficient *hTN*Ftg mice (supplementary material Fig. S3A,B), which suggested that the phenotype was already present at birth, prompting us to analyze their skeletons. Alcian Blue and Alizarin Red staining did not reveal any overwhelming developmental phenotypes (supplementary material Fig. S3C), but in situ hybridization revealed that the expression of collagen type I alpha 1 (*Col1a1*) was lower in the bones of RSK2-deficient *hTNF*tg mice (supplementary material Fig. S3D). To further describe the phenotype, we analyzed the expression of osteoblastic and osteocytic markers in entire bones from the four groups of mice. In situ hybridization at 6 weeks of age clearly confirmed the much lower expression of *Col1a1* only in the bones of RSK2-deficient *hTNF*tg mice (Fig. 5A). This observation was verified by quantitative real-time PCR analysis (Fig. 5B). In addition, although no differences in *Runx2* expression were detected (Fig. 5C), expression of two other osteoblast marker genes, namely osterix (Fig. 5D) and osteocalcin (Fig. 5E), was lower. Importantly, three osteocyte maker genes, phosphate-regulating gene with homologies to endopeptidases on the X chromosome (*Phex*; Fig. 5F), sclerostin (Fig. 5G) and dentin matrix acidic phosphoprotein 1 (*Dmp1*; Fig. 5E), were also strongly suppressed in the double mutant mice.

Increased osteoblast and osteocyte apoptosis in RSK2-deficient *hTNF*tg mice

TNF-α has been proposed to block bone formation by inducing apoptosis of osteoblastic cells (Gilbert et al., 2000; Jilka et al., 1998). The lower levels of expression of osteoblast and osteocyte markers in the bone of RSK2-deficient *hTNF*tg mice as well as fewer osteoblasts suggested that apoptosis of osteoblast was enhanced in these mice. To test this hypothesis, we performed TUNEL staining on sections of 6-week-old mice. As expected, there were more TUNEL-positive bone lining cells in *hTNF*tg mice, which were probably osteoblasts, and again RSK2 inactivation resulted in more apoptotic osteoblasts (Fig. 6A,B). Similarly, more TUNEL-positive cells were seen in the cortical bone of RSK2-deficient *hTNF*tg mice (Fig. 6C,D) suggesting an increased sensitivity of osteocytes lacking RSK2 to TNF-induced apoptosis. We next performed immunostaining for sclerostin, an osteocyte marker (Poole et al., 2005), to better analyze the osteocytic phenotype. Although a mild increase in the numbers of empty lacunae was observed in *hTNF*tg mice, numbers of empty lacunae dramatically increased in the bones of 6- and 10-week-old RSK2-deficient *hTNF*tg mice (Fig. 6E,F). These data suggest that deleting RSK2 renders osteoblasts and osteocytes more sensitive to TNF-induced cell death.

Cell autonomous increased sensitivity of RSK2-deficient osteoblasts to TNF-α-induced apoptosis

We and others have previously reported the essential cell-autonomous function of RSK2 in mediating osteoblast differentiation (David et al., 2005; Yang et al., 2004). We therefore hypothesized that the decrease in osteoblastogenesis observed in RSK2-deficient *hTNF*tg mice requires the cell-autonomous function of RSK2, which is further impaired by TNF-α in vivo. We first performed colony-forming unit (CFUs) experiments to determine the frequency of osteoblast progenitors present in the bone marrow of the various genotypes. RSK2 inactivation did not change the total numbers of colonies (data not shown) or the numbers of alkaline-phosphatase-positive colonies generated in vitro (Fig. 7A,B), clearly indicating that the osteoblastic phenotype was not caused by fewer osteoblastogenic progenitors.

The almost complete block in osteoblast differentiation observed in in vitro culture of primary osteoblasts lacking RSK2 (David et al., 2005) precluded any study of the effect of TNF-α on osteoblast differentiation in the absence of RSK2. However, we compared the growth curves of primary osteoblasts (POBs) isolated from the calvarias of wild-type, $Rsk2^{-/y}$, *hTNF*tg and *hTNF*tg;$Rsk2^{-/y}$ new-born mice. There were fewer growing POBs isolated from RSK2-deficient mice and *hTNF*tg mice lacking RSK2 than from wild-type and *hTNF*tg mice. A TUNEL assay was performed to determine whether differences in apoptosis could explain the variation. No difference in the numbers of apoptotic cells was found, which suggested a TNF-α-independent proliferative defect in POBs lacking RSK2 (Fig. 7C). Because TNF-α is a known inducer of osteoblasts apoptosis, we postulated that the increased sensitivity of osteoblastic cells to TNF-α-induced apoptosis in vivo was a cell autonomous defect. To test this hypothesis we cultured primary osteoblasts isolated from new-born calvarias of wild-type and RSK2-deficient mice at postnatal day (P) 5 in the presence or absence of exogenous TNF-α. A mild increase in the numbers of TUNEL-positive osteoblasts was seen in wild-type cells following TNF-α stimulation, but a significant ($P<0.001$) increase in

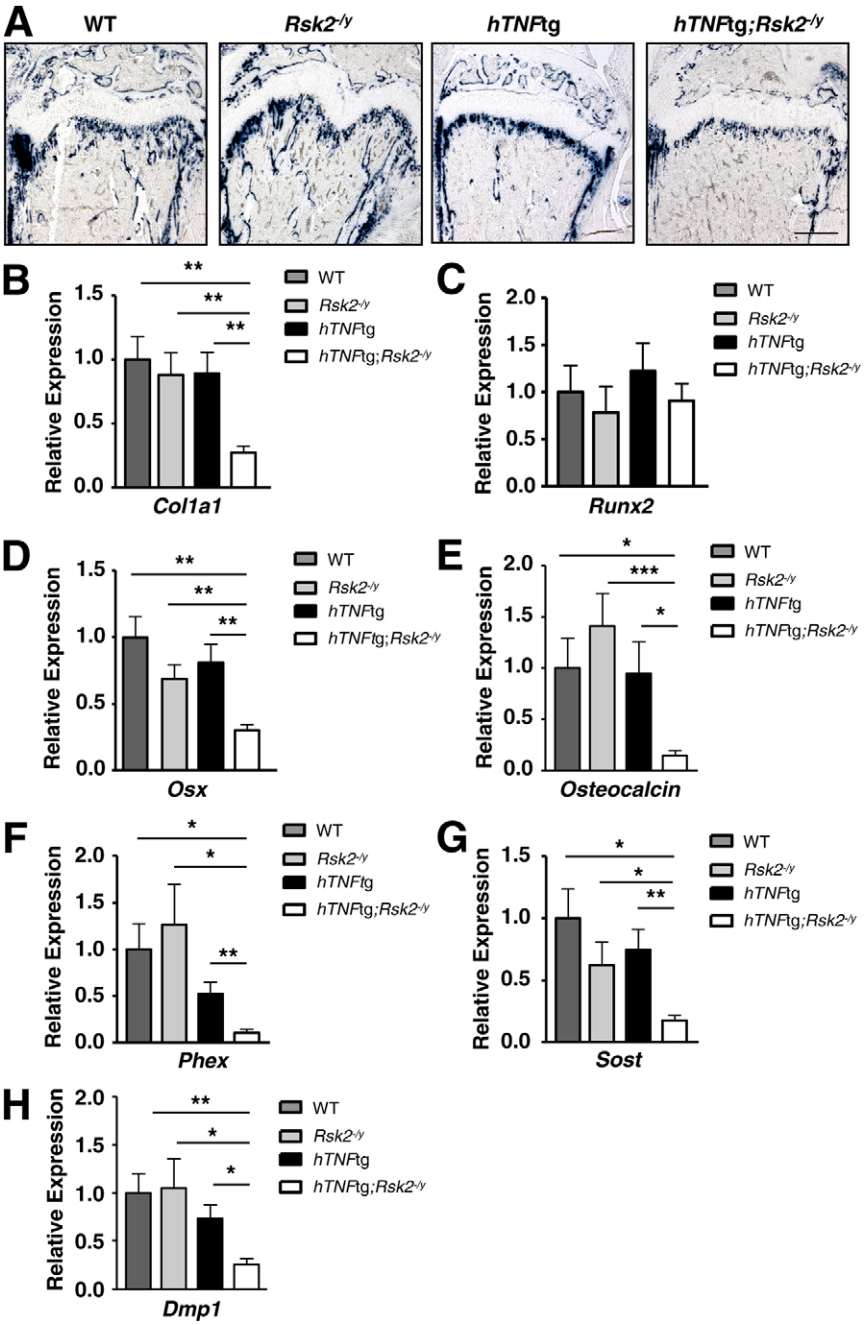

Fig. 5. Expression of osteoblast and osteocyte markers in long bones of RSK2-deficient *hTNF*tg mice. (**A**) In situ hybridization for Col1a1 expression in tibiae from 6-week-old males of the indicated genotypes. Scale bar: 500 μm. (**B–H**) Real-time PCR analysis of the expression of osteoblast and osteocyte markers in long bones of 6-week-old males (n=8–14 mice): (B) collagen type 1 alpha 1 (Col1a), (C) *Runx2*, (D) osterix (*Osx*), (E) osteocalcin, (F) phosphate-regulating gene with homologies to endopeptidases located on the X-chromosome (*Phex*), (G) sclerostin (*Sost*) and (H) dentin matrix protein 1 (*Dmp1*). Values are means ± s.e.m. *P<0.05, **P<0.01, ***P<0.001.

TNF-α-induced apoptosis was seen in RSK2-deficient cells (Fig. 7E,F). We next made use of a specific RSK2 inhibitor (Smith et al., 2005) to determine whether a direct inhibition of RSK2 could render wild-type osteoblasts as sensitive to TNF-α-induced apoptosis as RSK2-deficient cells. Although the treatment of RSK2-deficient primary osteoblasts with the specific RSK2 inhibitor did not change their response to TNF-α-induced apoptosis, it enhanced sensitivity to TNF-α-induced apoptosis in wild-type cells to an almost similar level as in the RSK2-deficient cells (Fig. 7G). We finally performed western blot analysis to determine whether TNF activation of RSK2 could directly be involved in the anti-apoptotic action of RSK2. Indeed, RSK2 was specifically activated by TNF-α stimulation in primary osteoblasts, as shown by the strong reactivity to an antibody directed against the phosphorylated form of RSK2. Moreover, the expected stimulation of JNK and ERK phosphorylation was seen in TNF-α-stimulated wild-type cells and was still occurred, although at a reduced level in the case of ERK, following RSK2 inactivation. Importantly, phosphorylation of the RSK2 substrate BAD (Bonni et al., 1999) that is required for its anti-apoptotic function was not found in RSK2-deficient osteoblasts stimulated with TNF-α (Fig. 7H).

Taken together our results establish that RSK2 is an antagonist mediator of TNF-α-induced apoptosis in the osteoblastic lineage and of recruitment of osteoclasts by osteoblasts, thereby protecting against TNF-induced bone loss.

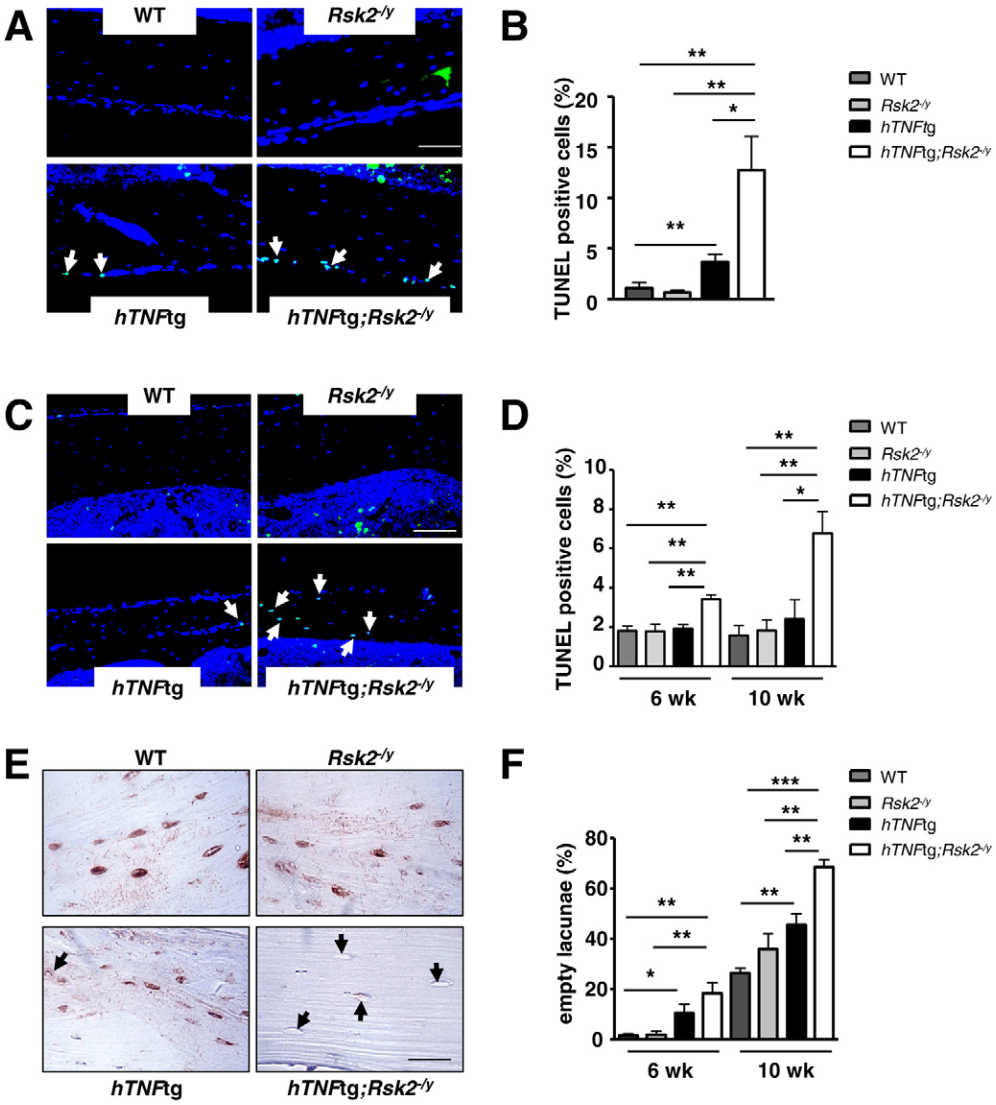

Fig. 6. Osteoblast and osteocyte apoptosis in *hTNF*tg;*Rsk2*$^{-/y}$ mice. (**A**) TUNEL staining of sections of cortical bone from tibiae of 6-week-old mice. Nuclei were counterstained with DAPI. White arrows indicate TUNEL-positive osteoblasts. Scale bar: 50 µm. (**B**) Quantification of TUNEL-positive cells relative to DAPI stained cells on the periosteum (n=5). (**C**) TUNEL staining of the cortex of tibiae of 10-week-old males. White arrows indicate TUNEL-positive osteocytes. Scale bar: 50 µm. (**D**) Quantification of TUNEL-positive osteocytes from 6- and 10-week-old male mice (n=3–5). (**E**) Immunohistochemical analysis of sclerostin expression in cortical bone (positive cells are stained in brown) of 10-week-old males. Empty lacunae are indicated by black arrows. Scale bar: 25 µm. (**F**) The percentage of empty lacunae in the cortical bone of 6- and 10-week-old males (n=4–5). Values are means ± s.e.m. *P<0.05, **P<0.01, ***P<0.001.

Discussion

This paper identifies the ERK- and PDK1-dependent kinase RSK2 as a negative regulator of TNF-α-induced systemic bone loss. RSK2 acts in osteoblasts to reduce their supportive osteoclastogenic activity and opposes the proapoptotic effect of TNF-α. Indeed, inactivation of RSK2 resulted in decreased bone mass, most probably because of non cell autonomous TNF-α-mediated recruitment of osteoclasts and drastic cell autonomous induction of apoptosis in osteoblast lineage cells.

TNF-α is a known regulator of bone remodeling. It decreases bone formation by osteoblasts and increases bone resorption by osteoclasts (David and Schett, 2010; Lam et al., 2000; Nanes, 2003). These effects are recapitulated in *hTNF*tg mice that develop a general age-dependent systemic osteopenia (Schett et al., 2003; Zaiss et al., 2010). Herein, we demonstrated that bone loss upon TNF-α expression leads to both increased osteoclast numbers and decreased osteoblast numbers in 10-week-old *hTNF*tg mice. Interestingly, inactivation of RSK2 not only resulted in an exacerbation of TNF-α-induced osteopenia, but also accelerated TNF-α-induced bone loss as shown by the drastic phenotype developing in 6-week-old mice, an age when no clear bone loss could be detected in either of the two parental lines, i.e. *hTNF*tg mice and RSK2-deficient mice. Thus, RSK2 inactivation sensitizes mice to the deleterious effects of TNF-α on bone. This is also illustrated by the more pronounced growth retardation and the earlier lethality observed in RSK2-deficient *hTNF*tg mice as well as the lower expression of collagen 1α1 seen in 3-day-old pups, and the earlier onset of clinical signs of arthritis (data not shown).

Both a TNF-α-mediated increase in osteoclasts and a decrease in osteoblasts were observed in the absence of RSK2. However, the osteoclast phenotype did not appear to be caused by a disturbance in the ratio of circulating RANKL/OPG or by a cell autonomous increased osteoclastogenesis but rather by a cell autonomous defect in the osteoblastic lineage that is a known local provider of RANKL in the bone. In accordance, we and others previously identified RSK2 as a kinase that positively regulates bone formation by osteoblasts. Indeed, in RSK2-deficient mice, no clear osteoclastic phenotype was observed in vivo, and in vitro differentiation of osteoclast progenitors in

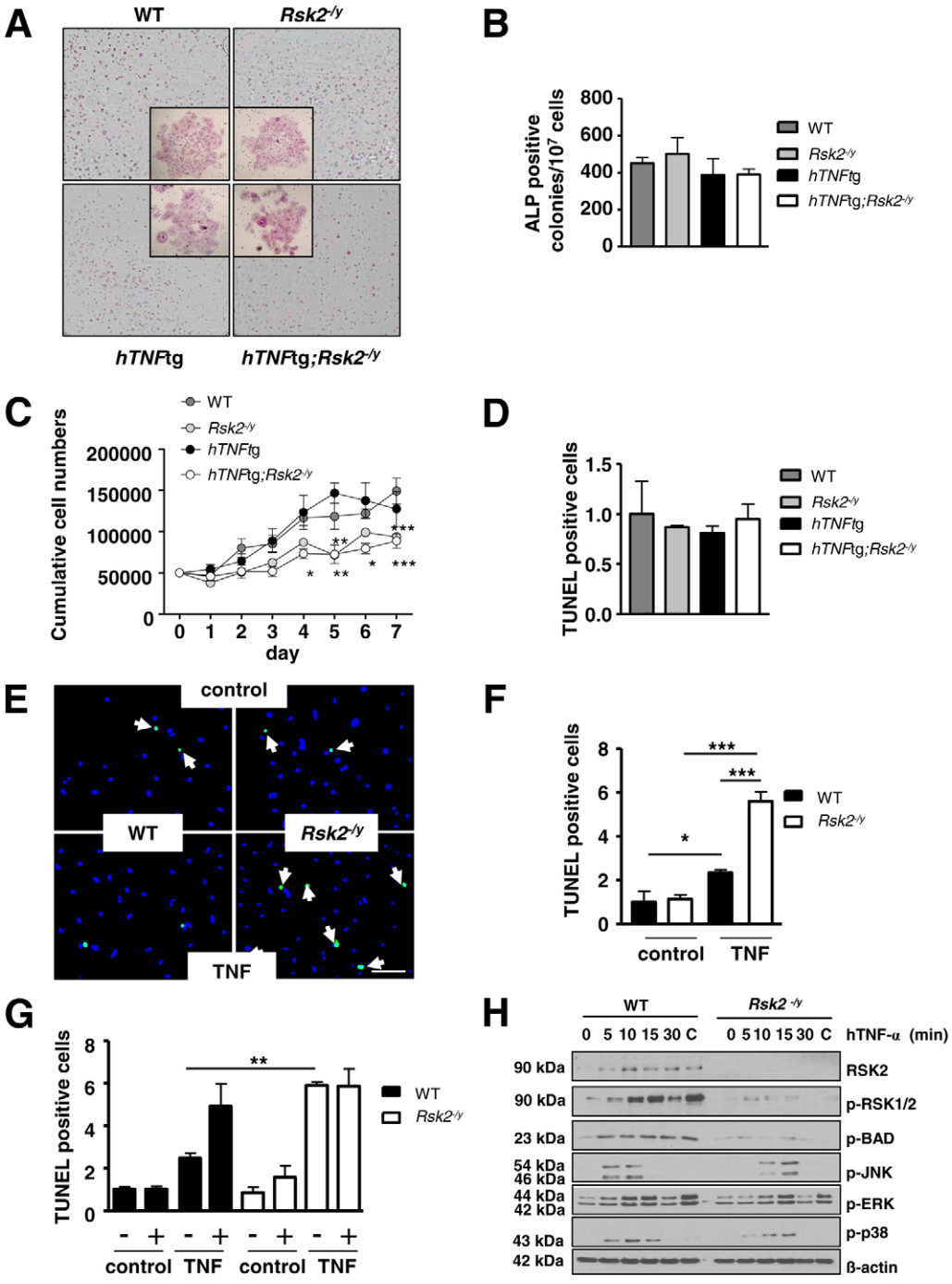

Fig. 7. Sensitivity of RSK2-deficient osteoblasts to TNF-induced apoptosis. (**A**) Alkaline phosphatase (ALP) staining of CFUs from cells of the bone marrow of the indicated genotype. The morphology of a single colony is shown in the inserts. (**B**) Quantification of ALP-positive colonies. (**C**) Growth curves of primary osteoblasts (POBs) of the indicated genotypes. (**D**) Quantification of TUNEL assay of the POBs after 3 days in culture. (**E**) TUNEL staining of primary osteoblasts isolated from WT and *Rsk2*$^{-/y}$ mice. Osteoblasts were cultured for 2 days in the absence (control) or presence of 10 ng/ml of hTNF-α (TNF). Scale bar: 50 µm. (**F**) Quantification of TUNEL-positive osteoblasts in the same culture condition. (**G**) Quantification of TUNEL-positive osteoblasts cultured in the absence or presence of hTNF-α and treated with an inhibitor of RSK2 (+) or untreated (−). (**H**) Western blot analysis of MAP-kinase and BAD activation in primary osteoblasts stimulated with 50 ng/ml hTNF-α for the indicated time. Stimulation with 20% FCS served as a control (C). Values are means ± s.e.m. of at least two independent experiments. *P<0.05, **P<0.01, ***P<0.001.

response to M-CSF and RANKL was similar to wild-type controls (David et al., 2005; Yang et al., 2004). We are now extending these observations to TNF-α-mediated osteoclastogenesis that was not affected by RSK2 inactivation in the presence of high or permissive doses of RANKL. Thus, the increased osteoclastogenesis seems to be indirect. It is probably in part a consequence of the increased supportive activity of the RSK2-deficient osteoblasts that express increased levels of RANKL in response to pro-osteoclastogenic stimuli including TNF-α. A second potential cause for the observed increase in osteoclast numbers in vivo is increased osteoblast and osteocyte apoptosis as illustrated by (1) the lower expression of markers for differentiation of osteoblasts and maturation of osteocytes, (2) the higher number of TUNEL-positive osteoblasts and osteocytes and (3) the more empty lacunae that we observed in both 6- and 10-week-old *hTNF*tg mice lacking RSK2. This hypothesis is in agreement with the proposed central role of osteocyte apoptosis in the initiation of bone remodeling, which would first recruit osteoclasts at the site of bone damage preceding osteoblast-mediated tissue repair (Bonewald, 2011; Jilka et al., 2007; Nakahama, 2010; Raggatt and Partridge, 2010). This model was clearly supported in mice expressing a conditional suicide gene in their osteocytes (Tatsumi et al., 2007) as well as by the capacity of osteocyte-derived apoptotic bodies to support in vitro and in

Journal of Cell Science

vivo osteoclastogenesis in a TNF-α-dependent manner (Kogianni et al., 2008).

In the case of *hTNF*tg mice lacking RSK2, osteoblast-mediated bone repair does not occur, as shown by the very strong decreased bone formation rate resulting from a combined decrease in the mineralizing surface and in the mineral apposition rate of both trabecular and periosteal bone. The osteoblastic phenotype is not due to lower numbers of osteogenic progenitors as demonstrated by the CFU assay but rather by the much lower numbers of differentiated osteoblasts that was further confirmed by analyzing the expression of osteoblastic markers in vivo, which, with the exception of RUNX2, were all found to be downregulated in *hTNF*tg mice lacking RSK2. Although the lower bone mass previously described in RSK2-deficient mice was not caused by a fewer osteoblasts but rather by a lower functionality of the cells (David et al., 2005; Yang et al., 2004), a higher bone mass due to higher osteoblast numbers was reported in mice lacking either TNF-α or the TNF-RI (Li et al., 2007), indicating that TNF-α primarily inhibits bone formation. Our data suggest that inactivating RSK2 sensitizes mice to the effect of TNF-α on bone inhibition. RSK2 acts as a protection against TNF-α-mediated inhibition of bone formation.

RSK2 is a growth-factor-regulated kinase that was reported to mediate cell cycle progression and cell proliferation in numerous cell types and organisms (Anjum and Blenis, 2008; Cho et al., 2005; David et al., 2005; Eisinger-Mathason et al., 2008; Lin et al., 2008; Romeo and Roux, 2011; Wang et al., 2010). We now report the reduced in vitro growth ability of osteoblast lacking RSK2. This phenomenon was independent of apoptosis and of the overexpression of TNF-α, as shown by the comparable growth curves of osteoblasts isolated from *hTNF*tg and wild-type mice on the one hand, and from the *Rsk2*$^{-/y}$ and RSK2-deficient *hTNF*tg mice on the other hand. Whether reduced proliferation in the absence of RSK2 and overexpression of TNF-α participate to the decrease osteoblasts numbers in vivo remains to be established. Indeed, some of the features of the RSK2-deficient osteoblasts in culture, such as an almost complete block of differentiation (David et al., 2005; Yang et al., 2004) (data not shown), do not reflect the in vivo phenotype of RSK2-deficient mice, indicating that a compensatory phenomenon might occur in vivo. By contrast, increased apoptosis sensitivity of osteoblasts and osteocytes is a clear feature of the bone phenotype of *hTNF*tg mice lacking RSK2. TNF-α was proposed to be an inducer of both osteocyte and osteoblast apoptosis (David and Schett, 2010; Nanes, 2003) and deleting RSK2 seems to sensitize these cells to TNF-mediated apoptosis. This finding is in agreement with publications that describe the anti-apoptotic roles of RSK2 (Anjum and Blenis, 2008; Anjum et al., 2005; Eisinger-Mathason et al., 2008; Kang et al., 2007; Lin et al., 2008; Peng et al., 2010) such as in transformed osteoblasts (David et al., 2005). Although we did not detect any change in the rate of apoptosis of unstimulated primary cultures of osteoblasts lacking RSK2 overexpressing or not hTNF-α compared with wild-type cells (David et al., 2005) (Fig. 7), RSK2-deficient osteoblasts were more sensitive to TNF-induced apoptosis. This phenotype was clearly RSK2 dependent as shown by the increased apoptosis in TNF-α-stimulated wild-type primary osteoblasts treated with a specific RSK2 inhibitor.

Among the proposed substrates of RSK2 are proteins regulating apoptosis such as p53, BimEL, IκBα, caspase 8 and BAD (Anjum et al., 2005; Cho et al., 2005; Dehan et al., 2009; Peng et al., 2010; Peng et al., 2011; Tan et al., 1999) that could mediate the protective effect of RSK2 on bone. We first confirmed in primary osteoblasts the activation of RSK2 by TNF-α previously reported in HeLa cells (Peng et al., 2010) and then we showed that activation of RSK2 leads to the phosphorylation of BAD on serine 112, a site necessary for its anti-apoptotic activity (Bonni et al., 1999). The decreased BAD phosphorylation observed in TNF-stimulated RSK2-deficient osteoblasts suggests that phosphorylated BAD is a mediator of the anti-apoptotic function of RSK2 in osteoblastic cells.

In conclusion, this work has identified RSK2 as a kinase activated by TNF-α in osteoblasts that exerts a negative regulatory loop on TNF-induced bone loss by protecting the osteoblastogenic lineage against TNF-α-induced apoptosis and slowing down the recruitment of osteoclasts by the osteoblasts. Thus, activators of RSK2 might be used as therapeutic treatments to block the adverse effects of TNF-α in bone in such conditions as systemic bone loss in rheumatoid arthritis.

Materials and Methods

Mice

All mice were maintained in a C57/Bl6 background in the animal facility of the University of Erlangen-Nuremberg. RSK2 knockout mice, previously described (David et al., 2005; Yang et al., 2004), were crossed with *hTNF*tg mice (strain Tg197) (Keffer et al., 1991). Because RSK2 is an X-linked gene, all experiments were carried out using 6- to 10-week-old male littermates. All animal experiments were approved by the local ethics committee.

Bone-marrow transplantation

For bone-marrow transplantation, recipient male *hTNF*tg mice (5 weeks old) were sublethally irradiated at 11 Gy, using orthovoltage irradiation (Stabilipan, Siemens) at 250 kV/15 mA/40 cm focus–surface distance at a dose rate of 1.15 Gy/minute. The next day, *hTNFtg* mice were injected intravenously with 5×10^6 donor bone marrow cells from wild-type or *Rsk2*$^{-/y}$ mice to reconstitute hematopoietic cells. The cells were applied in Medium 199 (Sigma) containing 5 ml 1 M HEPES buffer (Gibco), 5 ml (1 mg/ml) DNAse (Sigma) and 40 µl (50 mg/ml) gentamycin (Sigma).

Micro-computer tomography (microCT) imaging

MicroCT images of tibias were acquired as previously described (Böhm et al., 2009) on a laboratory cone-beam µCT scanner for ultra-high-resolution imaging (Wachsmuth and Engelke, 2004) developed at the Institute of Medical Physics of the University of Erlangen-Nuremberg, at 6 µm resolution (Skyscan 1174, Skyscan).

Histology

For Calcein labeling, mice were injected with 5 mg/kg body weight of green fluorescent Calcein (Sigma) 8 and 2 days before killing. The right tibia was fixed overnight in 4% formalin and then decalcified in 14% EDTA (Sigma) at 4℃ (the pH was adjusted to 7.2 by adding ammonium hydroxide; Sigma) until the bone was pliable. Serial paraffin sections (2 µm) from tibias were cut and stained for tartrate-resistant acid phosphatase (TRAP) to detect osteoclasts (2≥nuclei, TRAP positive) or used for TUNEL staining. For bone histomorphometry, left tibiae were fixed overnight in 4% formalin and then transferred to 70% ethanol. Undecalcified bones were embedded in methacrylate and 5 µm sections were cut. Unstained sections were used to measure fluorescent calcein-labeled bone surfaces at a wavelength of 495 nm. Toluidine Blue staining was performed for quantification of osteoblasts and von Kossa staining for bone mineralization. Analysis of all bone parameters was done using the OsteoMeasure histomorphometry system (OsteoMetrics Inc.).

ELISA

To determine the systemic levels of OPG and RANKL in the mice, blood was harvested from 6-week-old mice and serum was separated by centrifugation. Serum levels of RANKL and OPG were measured according to the instructions of the manufacturer (R&D Systems). For the detection of RANKL the serum was used at a 1:2 dilution; for OPG measurement the serum was used in a 1:10 dilution.

Immunohistology

Deparaffinized, ethanol-dehydrated tissue sections were heat in 0.1 M citrate buffer, pH 6 in a water bath (95℃, 15 min) for epitope retrieval, followed by

blocking of endogenous peroxidase with 3% H_2O_2. A primary antibody against murine sclerostin (R&D Systems) was used on tibia sections at 1:100 dilution followed by incubation with a biotinylated goat-anti-rabbit IgG secondary antibody (Vector Laboratories). Sections were incubated with the appropriate StreptABcomplex (Dako) using DAB-Chromogen (Dako) as chromogen, resulting in brown staining of antigen-expressing cells.

TUNEL assay

For determination of apoptosis, deparaffinized, ethanol-dehydrated bone sections or osteoblasts, grown on round coverslips were stained using the In Situ Cell Death Detection Kit (Roche Diagnostics) according to the manufacturer's protocol. Nuclei were counterstained with DAPI mounting solution (Vector Laboratories).

In situ hybridization

RNA in situ hybridization on paraffin sections of tibiae with digoxigenin-labeled antisense riboprobes specific for *Col1a1* was performed as previously described (Schmidl et al., 2006). Alkaline-phosphatase-conjugated anti-digoxigenin was incubated according to the manufacturer's protocol (Roche Diagnostics). Positive signals were visualized using BM Purple AP Substrate (Roche Diagnostics). Images were acquired using a Nikon Eclipse 80i microscope equipped with a Sony DXC-390P digital camera and NISElements BR2.20 software.

Alcian Blue and Alizarin Red staining of mouse skeletons

Preparation and staining of skeletons with Alcian Blue and Alizarin Red was performed as previously described (Hogan et al., 1994). P3.5 mice were killed with CO_2 and skin and internal organs were removed. The carcasses were fixed in 95% ethanol and stained with Alcian Blue (0.015% Alcian Blue 8GX, 20% acetic acid, 80% ethanol) for 12 hours. After washing in 95% ethanol for 3 hours, they were treated with 2% KOH for 1 day and stained with Alizarin Red (50 mg/l Alizarin Red sodium sulfate, 1% KOH) for 12 hours. The skeletons were further cleared with 1% KOH and 20% glycerol.

RNA isolation and real-time PCR

Total RNA from long bones was isolated using Trifast (Peqlab) according to the manufacturer's protocol. For homogenization of long bones a Precelly®24 Homogenisator (Peqlab) was used. After DNAse digestion, a total of 1 ng RNA was used for cDNA synthesis. Real-time PCR was performed using the following primers: for collagen 1a1 (*Col1a1*) 5′-CTGGCGGTTCAGGTCCAAT-3′ and 5′-TTCCAGGCAATCCACGAGC-3′; for *Runx2* 5′-TGTTCTCTGATCGCCTCA-GTG-3′ and 5′-CCTGGGATCTGTAATCTGACTCT-3′, for osterix (*Osx*) 5′-GGAGGCACAAAGAAGCCATACGC-3′ and 5′-TGCAGGAGAGAGGAGTC-CATTG-3′; for osteocalcin 5′-CTGACCTCACAGATCCCAAGC-3′ and 5′-TGGTCTGATAGCTCGTCACAAG-3′; for sclerostin (*Sost*) 5′-AGCCTTCAGG-AATGATGCCAC-3′ and 5′-CTTTGGCGTCATAGGGATGGT-3′; for *PHEX* 5′-ATTGCTGATAATGGGGGTCT-3′ and 5′-CTCCTGGCAGCTTCTGGTCT-3′; for dentin matrix protein-1 (*Dmp-1*) 5′-GTGCCCAAGATACCCCCAG-3′ and 5′GCATCCCTTCATCGAACTCA-3′; for *OPG* 5′-CTTGCCTTGATGGAGAG-CCT-3′ and 5′-TCGCTCGATTTGCAGGTCT-3′: for RANKL 5′-GTCTG-CAGCATCGCTCTGT-3′ and 5′-CCACAATGTGTTGCAGTTCC-3′.

Cell culture

Primary osteoblasts were isolated from calvariae of neonatal (4- to 6-day old) *Rsk2*$^{-/y}$ and wild-type mice as previously described (Jochum et al., 2000). Calvariae were digested sequentially in modified Eagle's medium type α (Gibco) containing 0.2% dispase II (Sigma) and 0.1% collagenase type IA (Sigma). Fractions were combined and cultured in α-MEM with 10% FCS (PAN) until subconfluency. Cells were then plated at a density of 10^4 cells/cm^2. For TUNEL assays, 10^4 cells were cultured on chamber slides and either pre-treated for 30 minutes with the RSK2 inhibitor SL0101-1 (Tocris) or left untreated and then stimulated with 10 ng/ml human TNF-α (R&D Systems) for 48 hours.

Osteoclast differentiation and coculture

Direct differentiation of osteoclast progenitors in response to MCSF and RANKL (R&D Systems) was performed as previously described (Böhm et al., 2009). Co-culture experiments for osteoclastogenesis were performed by stimulating the cells with 10^{-8} M 1α25$(OH_2)D_3$-dihydroxyvitamin D_3 and 10^{-7} M dexamethasone as previously described (Jochum et al., 2000). In both cases the efficacy of differentiation was evaluated by counting the multinucleated TRAP-positive osteoclasts formed in the culture using a TRAP staining kit (Sigma).

Colony-forming unit (CFU) assay

The colony-forming ability of bone marrow isolated from wild-type, *Rsk2*$^{-/y}$, *hTNF*tg and *hTNF*tg;*Rsk2*$^{y/-}$ mice was determined as follow: the bone marrow of two mice per genotype was isolated from femurs, tibiae and humeri. The bone marrow cells of each genotype were filtered and pooled. The erythrocytes were lysed and 1×10^7 cells were seeded in α-MEM medium (Gibco) with 15% FCS in three 15 cm dishes per condition. After 18 days the cells were fixed with 10% formalin and stained for alkaline phosphatase (ALP) activity (Millipore). The number of ALP-positive colonies was counted. The cells were subjected to Hematoxylin staining and the number of total colonies was determined.

Western blot analysis

Osteoblasts (5×10^4) were plated and serum-starved for 4 hours (α-MEM with 0.5% FCS). The cells were stimulated with 50 ng/ml human TNF-α (R&D Systems) for 5, 10, 15 or 30 minutes. No stimulation and 20% FCS for 5 minutes served as negative and positive control, respectively. TNF-α stimulation of osteoblasts was stopped using ice-cold PBS. Cells were lyzed in Laemmli buffer (Bio-Rad) and protein extracts were separated on a 12% sodium dodecyl sulphate polyacrylamide gel. Protein was transferred onto a nitrocellulose membrane using a semi-dry transfer chamber. The following antibodies were used for detection: anti-phosphorylated-p38, anti-phosphorylated-JNK, anti-phosphorylated-ERK, anti-phosphorylated-BAD (Cell Signaling), anti-RSK2 (Santa Cruz), anti-phosphorylated-RSK/2 (R&D Systems) and anti-β-actin (Sigma).

Statistical analysis

All statistical analyses were performed using GraphPadPrism software with Student's *t*-test or two-way ANOVA and are presented as means (± s.e.m.). *$P<0.05$, **$P<0.01$, ***$P<0.001$.

Acknowledgements

The authors thank Wolfgang Baum for taking care of the *hTNF*tg mice colony and Eugenia Schefler, Maria Gesslein, Isabell Schmidt and Cornelia Stoll for technical assistance.

Funding

This work was supported by the Deutsche Forschungsgemeinschaft Interdisziplinäres Zentrum für Klinische Forschung Erlangen [grant number A3 to G.S.]; Deutsche Forschungsgemeinschaft Ph.D. training grants [grant numbers GK592 to M.M.Z. and G.S., GK1660 to J.-P.D. and G.S.]; the Deutsche Forschungsgemeinschaft IMMUNOBONE [grant number SPP1468 to M.S., J.-P.D. and J.P.T.]; the European Commission FP7 project ADIPOA [grant number 2241719 to G.S. and J.-P.D.] and KINACEPT [grant number 222509 to G.S.]; and Boehringer Ingelheim Stiftung [to J.P.T.].

Supplementary material available online at
http://jcs.biologists.org/lookup/suppl/doi:10.1242/jcs.096008/-/DC1

References

Abu-Amer, Y., Erdmann, J., Alexopoulou, L., Kollias, G., Ross, F. P. and Teitelbaum, S. L. (2000). Tumor necrosis factor receptors types 1 and 2 differentially regulate osteoclastogenesis. *J. Biol. Chem.* **275**, 27307-27310.

Anjum, R. and Blenis, J. (2008). The RSK family of kinases: emerging roles in cellular signalling. *Nat. Rev. Mol. Cell Biol.* **9**, 747-758.

Anjum, R., Roux, P. P., Ballif, B. A., Gygi, S. P. and Blenis, J. (2005). The tumor suppressor DAP kinase is a target of RSK-mediated survival signaling. *Curr. Biol.* **15**, 1762-1767.

Böhm, C., Hayer, S., Kilian, A., Zaiss, M. M., Finger, S., Hess, A., Engelke, K., Kollias, G., Krönke, G., Zwerina, J. et al. (2009). The alpha-isoform of p38 MAPK specifically regulates arthritic bone loss. *J. Immunol.* **183**, 5938-5947.

Bonewald, L. F. (2011). The amazing osteocyte. *J. Bone Miner. Res.* **26**, 229-238.

Bonni, A., Brunet, A., West, A. E., Datta, S. R., Takasu, M. A. and Greenberg, M. E. (1999). Cell survival promoted by the Ras-MAPK signaling pathway by transcription-dependent and -independent mechanisms. *Science* **286**, 1358-1362.

Bruzzaniti, A. and Baron, R. (2006). Molecular regulation of osteoclast activity. *Rev. Endocr. Metab. Disord.* **7**, 123-139.

Charatcharoenwitthaya, N., Khosla, S., Atkinson, E. J., McCready, L. K. and Riggs, B. L. (2007). Effect of blockade of TNF-alpha and interleukin-1 action on bone resorption in early postmenopausal women. *J. Bone Miner. Res.* **22**, 724-729.

Cho, Y. Y., He, Z., Zhang, Y., Choi, H. S., Zhu, F., Choi, B. Y., Kang, B. S., Ma, W. Y., Bode, A. M. and Dong, Z. (2005). The p53 protein is a novel substrate of ribosomal S6 kinase 2 and a critical intermediary for ribosomal S6 kinase 2 and histone H3 interaction. *Cancer Res.* **65**, 3596-3603.

David, J. P. and Schett, G. (2010). TNF and bone. *Curr. Dir. Autoimmun.* **11**, 135-144.

David, J. P., Mehic, D., Bakiri, L., Schilling, A. F., Mandic, V., Priemel, M., Idarraga, M. H., Reschke, M. O., Hoffmann, O., Amling, M. et al. (2005). Essential role of RSK2 in c-Fos-dependent osteosarcoma development. *J. Clin. Invest.* **115**, 664-672.

Dehan, E., Bassermann, F., Guardavaccaro, D., Vasiliver-Shamis, G., Cohen, M., Lowes, K. N., Dustin, M., Huang, D. C., Taunton, J. and Pagano, M. (2009). betaTrCP- and Rsk1/2-mediated degradation of BimEL inhibits apoptosis. *Mol. Cell* **33**, 109-116.

Journal of Cell Science

Eisinger-Mathason, T. S., Andrade, J., Groehler, A. L., Clark, D. E., Muratore-Schroeder, T. L., Pasic, L., Smith, J. A., Shabanowitz, J., Hunt, D. F., Macara, I. G. et al. (2008). Codependent functions of RSK2 and the apoptosis-promoting factor TIA-1 in stress granule assembly and cell survival. *Mol. Cell* **31**, 722-736.

Gilbert, L., He, X., Farmer, P., Boden, S., Kozlowski, M., Rubin, J. and Nanes, M. S. (2000). Inhibition of osteoblast differentiation by tumor necrosis factor-alpha. *Endocrinology* **141**, 3956-3964.

Gilbert, L., He, X., Farmer, P., Rubin, J., Drissi, H., van Wijnen, A. J., Lian, J. B., Stein, G. S. and Nanes, M. S. (2002). Expression of the osteoblast differentiation factor RUNX2 (Cbfa1/AML3/Pebp2alpha A) is inhibited by tumor necrosis factor-alpha. *J. Biol. Chem.* **277**, 2695-2701.

Hofbauer, L. C., Lacey, D. L., Dunstan, C. R., Spelsberg, T. C., Riggs, B. L. and Khosla, S. (1999). Interleukin-1beta and tumor necrosis factor-alpha, but not interleukin-6, stimulate osteoprotegerin ligand gene expression in human osteoblastic cells. *Bone* **25**, 255-259.

Hogan, B., Beddington, R., Constantini, F. and Lacy, E. (1994). *Manipulating The Mouse Embryo: A Laboratory Manual*, 2nd edn. New York: Cold Spring Harbor Laboratory Press.

Jilka, R. L., Weinstein, R. S., Bellido, T., Parfitt, A. M. and Manolagas, S. C. (1998). Osteoblast programmed cell death (apoptosis): modulation by growth factors and cytokines. *J. Bone Miner. Res.* **13**, 793-802.

Jilka, R. L., Weinstein, R. S., Parfitt, A. M. and Manolagas, S. C. (2007). Quantifying osteoblast and osteocyte apoptosis: challenges and rewards. *J. Bone Miner. Res.* **22**, 1492-1501.

Jochum, W., David, J. P., Elliott, C., Wutz, A., Plenk, H., Jr, Matsuo, K. and Wagner, E. F. (2000). Increased bone formation and osteosclerosis in mice overexpressing the transcription factor Fra-1. *Nat. Med.* **6**, 980-984.

Kang, S., Dong, S., Gu, T. L., Guo, A., Cohen, M. S., Lonial, S., Khoury, H. J., Fabbro, D., Gilliland, D. G., Bergsagel, P. L. et al. (2007). FGFR3 activates RSK2 to mediate hematopoietic transformation through tyrosine phosphorylation of RSK2 and activation of the MEK/ERK pathway. *Cancer Cell* **12**, 201-214.

Karsenty, G., Kronenberg, H. M. and Settembre, C. (2009). Genetic control of bone formation. *Annu. Rev. Cell Dev. Biol.* **25**, 629-648.

Keffer, J., Probert, L., Cazlaris, H., Georgopoulos, S., Kaslaris, E., Kioussis, D. and Kollias, G. (1991). Transgenic mice expressing human tumour necrosis factor: a predictive genetic model of arthritis. *EMBO J.* **10**, 4025-4031.

Kogianni, G., Mann, V. and Noble, B. S. (2008). Apoptotic bodies convey activity capable of initiating osteoclastogenesis and localized bone destruction. *J. Bone Miner. Res.* **23**, 915-927.

Lam, J., Takeshita, S., Barker, J. E., Kanagawa, O., Ross, F. P. and Teitelbaum, S. L. (2000). TNF-alpha induces osteoclastogenesis by direct stimulation of macrophages exposed to permissive levels of RANK ligand. *J. Clin. Invest.* **106**, 1481-1488.

Li, Y., Li, A., Strait, K., Zhang, H., Nanes, M. S. and Weitzmann, M. N. (2007). Endogenous TNFalpha lowers maximum peak bone mass and inhibits osteoblastic Smad activation through NF-kappaB. *J. Bone Miner. Res.* **22**, 646-655.

Lin, J. X., Spolski, R. and Leonard, W. J. (2008). Critical role for Rsk2 in T-lymphocyte activation. *Blood* **111**, 525-533.

Lu, X., Gilbert, L., He, X., Rubin, J. and Nanes, M. S. (2006). Transcriptional regulation of the osterix (Osx, Sp7) promoter by tumor necrosis factor identifies disparate effects of mitogen-activated protein kinase and NF kappa B pathways. *J. Biol. Chem.* **281**, 6297-6306.

Marques Pereira, P., Schneider, A., Pannetier, S., Heron, D. and Hanauer, A. (2010). Coffin-Lowry syndrome. *Eur. J. Hum. Genet.* **18**, 627-633.

Nakahama, K. (2010). Cellular communications in bone homeostasis and repair. *Cell. Mol. Life Sci.* **67**, 4001-4009.

Nanes, M. S. (2003). Tumor necrosis factor-alpha: molecular and cellular mechanisms in skeletal pathology. *Gene* **321**, 1-15.

Pacifici, R. (2008). Estrogen deficiency, T cells and bone loss. *Cell. Immunol.* **252**, 68-80.

Peng, C., Cho, Y. Y., Zhu, F., Xu, Y. M., Wen, W., Ma, W. Y., Bode, A. M. and Dong, Z. (2010). RSK2 mediates NF-kappaB activity through the phosphorylation of IkappaBalpha in the TNF-R1 pathway. *FASEB J.* **24**, 3490-3499.

Peng, C., Cho, Y. Y., Zhu, F., Zhang, J., Wen, W., Xu, Y., Yao, K., Ma, W. Y., Bode, A. M. and Dong, Z. (2011). Phosphorylation of caspase-8 (Thr-263) by ribosomal S6 kinase 2 (RSK2) mediates caspase-8 ubiquitination and stability. *J. Biol. Chem.* **286**, 6946-6954.

Plotkin, L. I., Weinstein, R. S., Parfitt, A. M., Roberson, P. K., Manolagas, S. C. and Bellido, T. (1999). Prevention of osteocyte and osteoblast apoptosis by bisphosphonates and calcitonin. *J. Clin. Invest.* **104**, 1363-1374.

Poole, K. E., van Bezooijen, R. L., Loveridge, N., Hamersma, H., Papapoulos, S. E., Löwik, C. W. and Reeve, J. (2005). Sclerostin is a delayed secreted product of osteocytes that inhibits bone formation. *FASEB J.* **19**, 1842-1844.

Raggatt, L. J. and Partridge, N. C. (2010). Cellular and molecular mechanisms of bone remodeling. *J. Biol. Chem.* **285**, 25103-25108.

Roggia, C., Gao, Y., Cenci, S., Weitzmann, M. N., Toraldo, G., Isaia, G. and Pacifici, R. (2001). Up-regulation of TNF-producing T cells in the bone marrow: a key mechanism by which estrogen deficiency induces bone loss in vivo. *Proc. Natl. Acad. Sci. USA* **98**, 13960-13965.

Romeo, Y. and Roux, P. P. (2011). Paving the way for targeting RSK in cancer. *Expert Opin. Ther. Targets* **15**, 5-9.

Schett, G. and David, J. P. (2010). The multiple faces of autoimmune-mediated bone loss. *Nat. Rev. Endocrinol.* **6**, 698-706.

Schett, G., Redlich, K., Hayer, S., Zwerina, J., Bolon, B., Dunstan, C., Görtz, B., Schulz, A., Bergmeister, H., Kollias, G. et al. (2003). Osteoprotegerin protects against generalized bone loss in tumor necrosis factor-transgenic mice. *Arthritis Rheum.* **48**, 2042-2051.

Schmidl, M., Adam, N., Surmann-Schmitt, C., Hattori, T., Stock, M., Dietz, U., de Crombrugghe, B., Pöschl, E. and von der Mark, K. (2006). Twisted gastrulation modulates bone morphogenetic protein-induced collagen II and X expression in chondrocytes in vitro and in vivo. *J. Biol. Chem.* **281**, 31790-31800.

Sfikakis, P. P. (2010). The first decade of biologic TNF antagonists in clinical practice: lessons learned, unresolved issues and future directions. *Curr. Dir. Autoimmun.* **11**, 180-210.

Smith, J. A., Poteet-Smith, C. E., Xu, Y., Errington, T. M., Hecht, S. M. and Lannigan, D. A. (2005). Identification of the first specific inhibitor of p90 ribosomal S6 kinase (RSK) reveals an unexpected role for RSK in cancer cell proliferation. *Cancer Res.* **65**, 1027-1034.

Tan, Y., Ruan, H., Demeter, M. R. and Comb, M. J. (1999). p90(RSK) blocks bad-mediated cell death via a protein kinase C-dependent pathway. *J. Biol. Chem.* **274**, 34859-34867.

Tatsumi, S., Ishii, K., Amizuka, N., Li, M., Kobayashi, T., Kohno, K., Ito, M., Takeshita, S. and Ikeda, K. (2007). Targeted ablation of osteocytes induces osteoporosis with defective mechanotransduction. *Cell Metab.* **5**, 464-475.

Teitelbaum, S. L. and Ross, F. P. (2003). Genetic regulation of osteoclast development and function. *Nat. Rev. Genet.* **4**, 638-649.

Thomson, B. M., Mundy, G. R. and Chambers, T. J. (1987). Tumor necrosis factors alpha and beta induce osteoblastic cells to stimulate osteoclastic bone resorption. *J. Immunol.* **138**, 775-779.

Wachsmuth, L. and Engelke, K. (2004). High-resolution imaging of osteoarthritis using microcomputed tomography. *Methods Mol. Med.* **101**, 231-248.

Wang, R., Jung, S. Y., Wu, C. F., Qin, J., Kobayashi, R., Gallick, G. E. and Kuang, J. (2010). Direct roles of the signaling kinase RSK2 in Cdc25C activation during Xenopus oocyte maturation. *Proc. Natl. Acad. Sci. USA* **107**, 19885-19890.

Yang, X., Matsuda, K., Bialek, P., Jacquot, S., Masuoka, H. C., Schinke, T., Li, L., Brancorsini, S., Sassone-Corsi, P., Townes, T. M. et al. (2004). ATF4 is a substrate of RSK2 and an essential regulator of osteoblast biology; implication for Coffin-Lowry Syndrome. *Cell* **117**, 387-398.

Zaiss, M. M., Frey, B., Hess, A., Zwerina, J., Luther, J., Nimmerjahn, F., Engelke, K., Kollias, G., Hünig, T., Schett, G. et al. (2010). Regulatory T cells protect from local and systemic bone destruction in arthritis. *J. Immunol.* **184**, 7238-7246.

Zhang, Y. H., Heulsmann, A., Tondravi, M. M., Mukherjee, A. and Abu-Amer, Y. (2001). Tumor necrosis factor-alpha (TNF) stimulates RANKL-induced osteoclastogenesis via coupling of TNF type 1 receptor and RANK signaling pathways. *J. Biol. Chem.* **276**, 563-568.

Journal of Cell Science

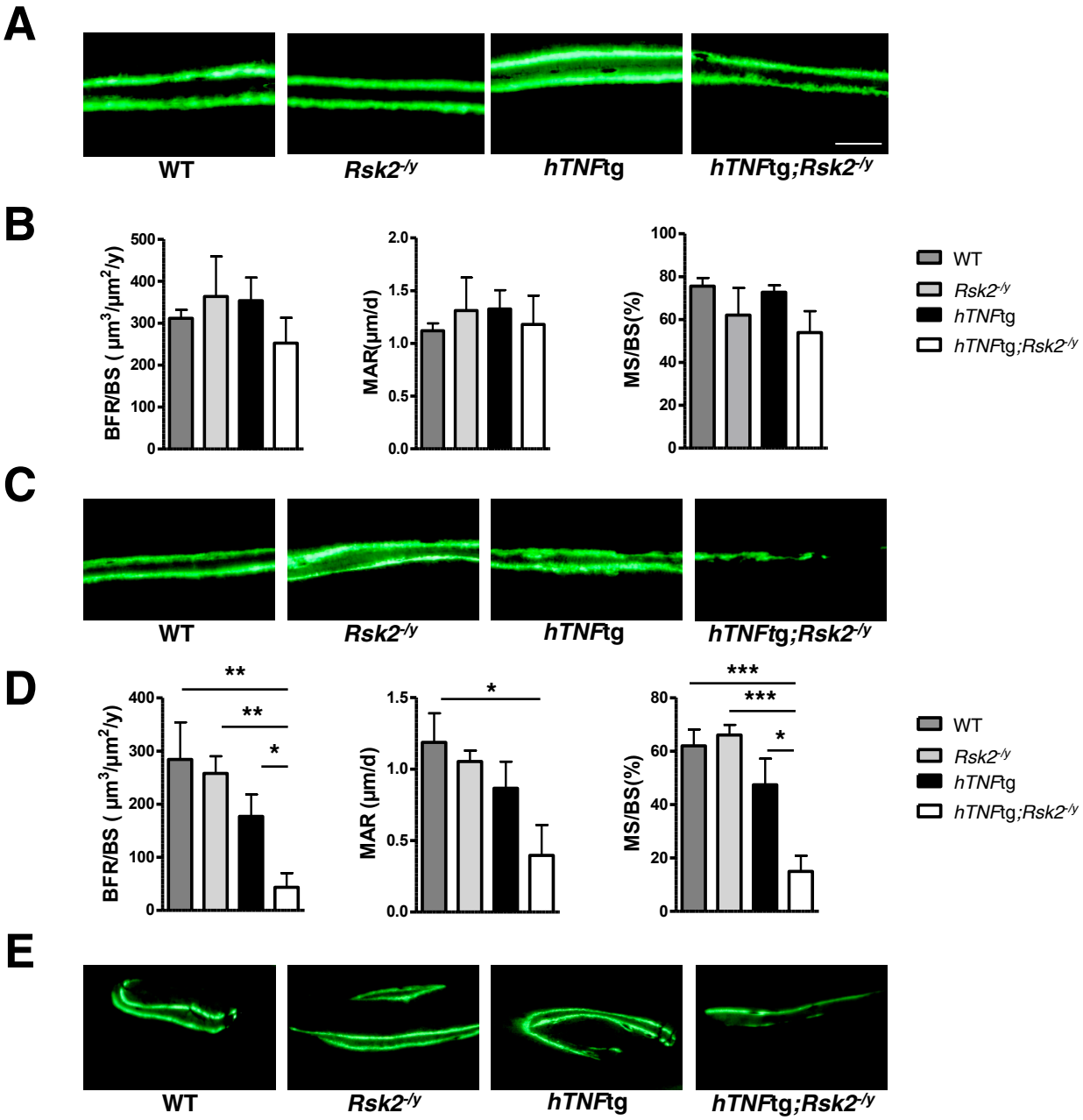
A
WT
Rsk2-/y
hTNFtg
hTNFtg;Rsk2-/y
B
BFR/BS (μm3/μm2/y)
MAR(μm/d)
MS/BS(%)
WT
Rsk2-/y
hTNFtg
hTNFtg;Rsk2-/y
C
WT
Rsk2-/y
hTNFtg
hTNFtg;Rsk2-/y
D
BFR/BS (μm3/μm2/y)
MAR (μm/d)
MS/BS(%)
WT
Rsk2-/y
hTNFtg
hTNFtg;Rsk2-/y
E
WT
Rsk2-/y
hTNFtg
hTNFtg;Rsk2-/y
F
BFR/BS (μm3/μm2/y)
MAR (μm/d)
MS/BS(%)
WT
Rsk2-/y
hTNFtg
hTNFtg;Rsk2-/y

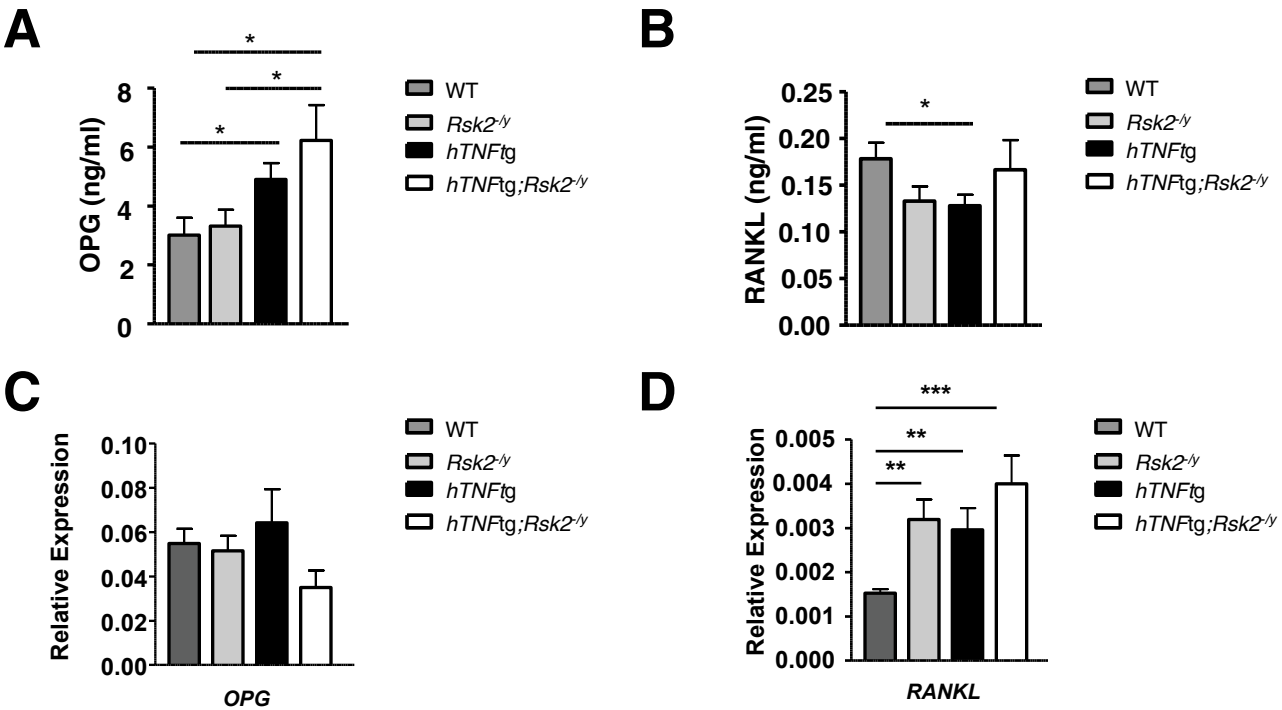
A
OPG (ng/ml)
0
2
4
6
8
*
*
*
WT
Rsk2-/y
hTNFtg
hTNFtg;Rsk2-/y
B
RANKL (ng/ml)
0.00
0.05
0.10
0.15
0.20
0.25
*
WT
Rsk2-/y
hTNFtg
hTNFtg;Rsk2-/y
C
Relative Expression
0.00
0.02
0.04
0.06
0.08
0.10
OPG
WT
Rsk2-/y
hTNFtg
hTNFtg;Rsk2-/y
D
Relative Expression
0.000
0.001
0.002
0.003
0.004
0.005
***
**
**
RANKL
WT
Rsk2-/y
hTNFtg
hTNFtg;Rsk2-/y

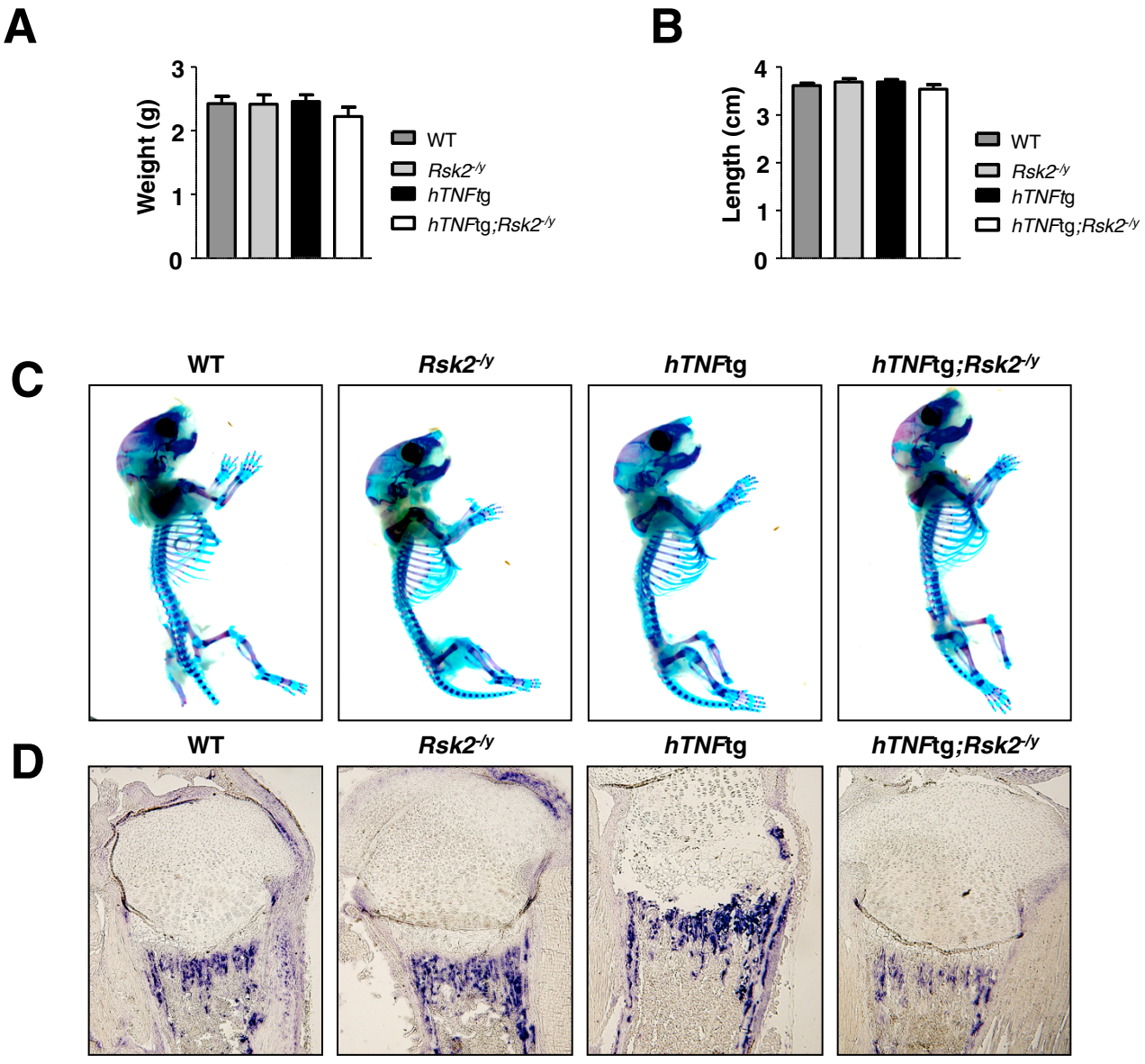
A
Weight (g)
3
2
1
0
WT
Rsk2-/y
hTNFtg
hTNFtg;Rsk2-/y
B
Length (cm)
4
3
2
1
0
WT
Rsk2-/y
hTNFtg
hTNFtg;Rsk2-/y
C
WT
Rsk2-/y
hTNFtg
hTNFtg;Rsk2-/y
D
WT
Rsk2-/y
hTNFtg
hTNFtg;Rsk2-/y